THE UNIVERSITY OF ALABAMA IN HUNTSVILLE

Huntsville, Alabama 35899

FINAL TECHNICAL REPORT

Contract NAS8-33731

By

J. E. Rush

Principal Investigator

Prepared for

George C. Marshall Space Flight Center
National Aeronautics and Space Administration
Marshall Space Flight Center, Alabama 35812

FINAL TECHNICAL REPORT

CONTAINERLESS PROCESSING TECHNOLOGY ANALYSIS

NASA CONTRACT NAS8-33731

by J. E. Rush, Principal Investigator

I. INTRODUCTION

This report covers research on acoustic levitation, air-jet levitation, and heat transfer from molten samples. Although the work on these topics was not completely sequential, they are separated in this report for clarity. The performance period was May 8, 1980 to August 31, 1982.

The thrust of this research was toward obtaining a better understanding and improving the quality of containerless processing systems of interest to Marshall Space Flight Center (MSFC). Such systems have application to the study and processing of materials in situations in which contact with a container must be avoided, and have potential application in both ground-based and orbiting laboratories. An overview of the general subject of containerless processing is given by Naumann and Herring (1). Typical applications of the systems studied here are in the development and study of glasses from materials which normally crystallize upon cooling.

In addition to the reports which have resulted from this work and which are identified in the following sections, the PI gave presentations on this work at the Space Sciences Laboratory, MSFC; a

Materials Research Society Symposium (see Appendix B); the University of the South Sigma Xi Chapter; the University of Alabama (Tuscaloosa); and The University of Alabama in Huntsville.

II. ACOUSTIC LEVITATION

A. Background

A single-axis acoustic levitator has been under study and development for several years under NASA sponsorship, the primary contractor being Intersonics, Inc. The work of this report has been primarily in support of, and in addition to, that of Intersonics. The Principal Investigator (PI) is indebted to Dr. Roy Whymark and Dr. Charles Rey of Intersonics for their cooperation in sharing information during the course of this research.

The acoustic levitator utilizes a high-intensity standing-wave sound field to levitate or position small (1 cm or less) objects. The basic device was designed by St. Clair (2) in 1940 for a completely different purpose. Current levitator designs are available in reports from Intersonics, Inc. The basic theory for employing high-intensity sound sources for levitation was worked out by King (3) in 1934, based on earlier work by Rayleigh.

The PI had done work related to the levitator prior to the award of this contract, first as a NASA/ASEE Summer Faculty Fellow at MSFC (1979) and later as a physicist on a related contract. The fellowship involved experimental work relative to the causes of problems in spot-heating samples in the levitator at 1 g, and is summarized in a final report (4) and in the proceedings of a symposium (5). Earlier work on the levitator was reported by Oran, et al. (6), and by Whymark (7).

The work following the fellowship was directed at obtaining a better theoretical understanding of the failure of spot heating. It turned out that quite a bit of related research had been done in other contexts, primarily involving the effect of acoustic fields on heat transfer from cylinders. Most of the pertinent references are contained in a review article by Richardson (8). The significant effect noted by these authors is a dramatic increase in heat transfer from cylinders in air when placed in an acoustic field of 140 db or greater.

While several explanations for the enhanced heat transfer rate have been proposed and the definitive answer has not been given, it is clear (9) that the acoustic field causes the laminar flow of gravitational convection to become turbulent, and this turbulence is correlated with the drastically increased rate of heat transfer. It was this turbulence which caused spot-heated samples to be lost from the 170 db acoustic field in the laboratory. The turbulence, however, is not manifest in acoustic fields with unheated samples. The fact that neither heating nor high-intensity sound, independently, produce significant turbulence, while the combination does, is not particularly surprising because of the nonlinearity of the equations at the intensities employed for levitation. Indeed, the nonlinearity is basic to the levitation process (see the equation for the mean sound-pressure level derived by King, Ref. 3, p. 215).

A summary of the published results on heat transfer in acoustic fields, including a brief analysis of each paper, is available from the PI. Also available are 16 mm motion-picture films showing the behavior of samples at 1 g, including the effect of heating, and plots of dc

(time averaged) pressure, ac pressure, and temperature in the sound field, with and without spot-heated samples.

B. Further Studies of Heat Transfer in Acoustic Fields

Because no definitive conclusions about the mechanisms for heat transfer in acoustic fields had been reached in the published literature, and because the parameter space involved in our levitation work had not been explored by other authors, it was considered advisable to carry out further studies of the phenomenon. The apparatus consisted of a very small cylindrical solenoid of Kanthal wire coated with a nonconducting material to form a 1.0 cm long cylinder with a diameter of 0.25 cm. The cylinder (several similar ones were used) was attached to nichrome wire and rigidly supported in the sound field at a velocity antinode in the standing waves.

Detailed measurements were made of the heat transfer rate in thermal equilibrium for cylinder temperatures up to 700°C and sound pressure levels (SPL) up to 170 db. Higher SPL values were available from the apparatus but could not be accurately measured. An estimated SPL of 178 db was observed.

Further details of these measurements, results, and comparison with published papers, are contained in an interim report which is made Appendix A of this final report. Note that Appendix A has a self-contained list of references.

C. Analysis of Behavior of Sample in Acoustic Field at Low G

At the request of R. Naumann of MSFC, the PI assisted in the analysis of results of a single-axis levitator experiment on the

SPAR-VIII flight (Space Processing Applications Rocket). The experiment was No. 74-42/2, flown on November 18, 1980. A preliminary analysis had already been carried out by C. Rey of Intersonics, Inc. The additional analysis was done by the PI and by C. F. Schafer of MSFC, with the assistance of R. L. Holland of MSFC. The results are presented in a NASA Technical Memorandum (10).

In addition to the experiment analysis and recommendations for improvement in future SPAR flights, the memorandum contains unpublished results on the radial properties of the sound field in an acoustic levitator, an extension of the work of King (3), done by the PI. Experimental work on acoustic streaming in the sound field of the levitator was also carried out by the PI in collaboration with C. F. Schafer and with W. K. Stephens of UAH. This work was not completed because of more pressing matters, but preliminary results, including photographs and 16 mm film, are available from the PI.

Copies of the NASA Technical Memorandum are available from the PI, as well as from the customary sources.

D. Other Work on Acoustic Levitation

In connection with the work discussed in Sections A-C, several related measurements were made, some of which are described in Appendix A.

A frequency analysis of the acoustic driver and the standing-wave field was made to facilitate an understanding of the nature of the field, and the results are in Appendix A. A study was also made of the lateral force on a small sphere, in connection with the analysis of

SPAR-VIII. The results of this study are contained in laboratory notebooks available from the PI.

III. AIR-JET LEVITATION

A. Background

The technical monitor for the initial work on acoustic levitation was W. A. Oran of MSFC. Following Dr. Oran's assignment to NASA Headquarters in September 1980, the technical monitor has been Dr. E. C. Ethridge of MSFC. All work by the PI on the air-jet levitator was done under Dr. Ethridge. The work was initially begun at the request of Dr. R. J. Naumann of MSFC.

A constricted-tube gas-flow levitator was developed at MSFC by Berge, Oran, and Theiss (11). The device consists of a quartz tube with a constriction introduced by melting and stretching (tubes were prepared by R. Smith, glassblower at UAH); a source of compressed air or gas; and a furnace for heating the air before it passes through the tube. By means of this device, Berge, et al., were able to levitate a spherical sample with the tube upright or inverted, and to heat the sample to temperatures greater than 1300°C.

The only results in the open literature directly related to this device were by Schmidt and Springer (12), involving a sphere in a diffuser, and they are not particularly useful for the air-jet (or gas-flow) levitator. There is, however, an extensive literature on spheres in tubes (see references in Appendix B).

The PI was asked to predict the behavior of samples in the levitator in a low-g environment.

B. Behavior of Samples in Air-Jet Levitator in Low G

The experimental parameters involved in understanding the behavior of the air-jet levitator are:

(a) flow rate of air or gas

(b) pressures in tube

(c) relative diameters of tube and constriction of sample

(d) angle and shape of constriction

(e) net force on sample at different positions in tube

(f) viscosity of air or gas

In order to predict the behavior of samples at low g, a study was made in which (b) and (e) were measured as (a), (c), and (d) were varied. The effect of (f) can be calculated from the Reynolds number.

The results of these measurements were presented at the Materials Research Society Symposium, "Materials Processing in the Reduced Gravity Environment of Space," Boston, November 16-18, 1981, with W. K. Stephens of UAH and E. C. Ethridge of MSFC. They are given in Appendix B, which is a copy of the paper which was presented. The conclusion is that the levitator should work as a positioning device at low g, but that care must be taken to regulate flow rates so that the molten sample never touches the tube. The development of the device for low g will thus require a careful study of flow rates vs. temperature, in a low gravity environment, to maintain sample stability.

C. Behavior of Samples in the Laboratory

Studies were also made of sample behavior in the laboratory at 1 g, and some of the results are contained in Appendix B. It is possible to

do a theoretical analysis of the air-jet levitator for laminar flow with a precisely defined geometry, and such an analysis would be quite similar to flow-meter theory. However, the flow is not laminar in the actual levitation experiments, and the academic interest of such an analysis hardly seems appropriate in the context of developing working devices.

The furnace arrangement built by Berge, Oran, and Theiss was redesigned and rebuilt by the PI with the help of R. Eakes of UAH, and is available for continued work at 1 g.

IV. HEAT TRANSFER FROM A MOLTEN SAMPLE

A. Background

The basic problem involved in this part of the project was to develop a computer model for the temperature distribution, as a function of position and time, in a small spherical drop of material which is cooling by conduction (in the material) and radiation. The material is neither opaque nor fully transparent. This problem is related to the processing of samples in drop tubes, on stings, etc.

The problem described above has never been solved. However, there are several simpler, related problems that have been solved approximately. The subject is discussed generally in a review article by Viskanta and Anderson (13). The basic problems of radiative transfer are presented by Chandrasekhar (14).

Some steady-state problems for which approximate solutions are available are

1) a gray spherical shell with no conduction (15-17);

2) a special nongray spherical shell with no conduction (18);

3) a gray spherical shell with radiation and conduction (19, 20);

4) conduction with no radiation (21).

Time-dependent problems which have been considered are

5) cooling of a spherical gray gas with no conduction (22, 23);

6) conduction in a sphere with no radiation (24).

B. Theoretical Model

In order to simplify use of the word processor for this report, we modify the conventional notation somewhat. Some pertinent variables in the problem are

u - energy density

$\underline{q}$ - heat flux vector

t - time

D - density

c - specific heat

T - temperature (absolute)

$\underline{f}$ - frequency of radiation

k - thermal conductivity

K - linear radiative absorptivity (depends on f)

n - index of refraction (depends on f)

The energy conservation equation is then

$$du/dt = - \text{div } q$$

where, for this section, d implies partial differentiation. Then from

$$\underline{q} = - k \text{ grad } T + \underline{F}$$

and $u = DcT$

we get

$$Dc\ dT/dt = \text{div}\ (k\ \text{grad}\ T) - \text{div}\ \underline{F}$$

which, with spherical symmetry, becomes

$$Dc\ dT/dt = r^{-2}\ \frac{d}{dr}\ (kr^2 dT/dr - r^2 F)$$

where F is the radial component of $\underline{F}$ and r is the radial coordinate.

The problem of the distribution of radiant energy for a given temperature distribution was solved by Chandrasekhar (14). The term div $\underline{F}$ can be represented as

$$\text{div}\ \underline{F} = \int_0^\infty K(f)[4\pi n^2(f)I(f) - G(f)]df$$

where I(f) is the blackbody distribution function and G(f) is the contribution from absorption in each small volume of material. The expression for div $\underline{F}$ in terms of temperature is given by Viskanta and Lall (22) in terms of exponential integral functions.

For the simplest case, we assume that c, k, K, and n are constant. Then we can change to dimensionless variables

$$x = r/r_o$$

$$w = xT/T_o$$

$$t^* = t/(Dc/KBT_o^3)$$

$$N = kK/BT_o^3$$

$$s = t^*\ N/(Kr_o)^2,$$

where r_o is the spherical boundary, T_o is the initial temperature, and B is the Stefan-Boltzmann constant. Then we get

$$du/ds = d^2u/dx^2 - H$$

where H is an integral representing the flux, which depends on position and temperature.

If we define

$$y = Kr$$

so that $x = y/y_o$

we find

$$H = y(4E'-G')$$

where $E' = (T/T_o)^4$

and $G' = G/BT_o^4$

with G the integral over frequency of G(f). Viskanta and Lall get for G,

$$G = (2/y) \int_o^{yo} E'[E_1 (|y-y'|) - E_1(y + y')] \, y'dy'$$

where E_1 is the exponential integral function.

The basic equation is thus an integro-differential equation of the parabolic type. We have explored a variety of possibilities for

approximate solutions to this equation, and finally settled on a direct computer approach using finite differences and numerical integration.

The most significant approximations which have been made are taking k independent of T and taking K independent of f. Relaxing the first restriction would make the calculation slightly more complicated, but the equation is already strongly nonlinear because of the flux integral, which is not small, so it would be a minor complication. Relaxing the second restriction is quite a serious matter.

Whether or not the second approximation is reasonable depends on the shape of the absorption curve for a given material in the vicinity of the blackbody peak. The position of the peak follows from Wien's displacement law

$$\ell_{max} T = 2898 \ \mu m\text{-}K$$

for wavelength ℓ. For the temperature range 2000 K to 3000 K, this gives ℓ_{max} from 1.5 to 1 microns. We have as yet no data on K for liquid alumina, but for solid alumina the transmittance is essentially uniform from 0.2 to 5 microns. To this extent the approximation of constant K for alumina ($A\ell_2O_3$) is a good one. For each additional substance of interest, the approximation must be reconsidered.

From an analysis of energy transfer at the spherical surface, it would appear that the appropriate boundary condition is

$$dT/dr = 0 \text{ at } r_o.$$

However, this gives

$$dw/dx = T/T_o \text{ at } r_o,$$

which is impracticable. A relatively minor modification is

$$dw/dx = 0 \text{ at } r_o$$

which gives

$$dT/dr = - T/r_o \text{ at } r_o.$$

Starting in thermal equilibrium at t = 0, we also expect

$T = T_o$ for r between 0 and r_o, but this gives a null solution, so we have chosen

$$T = T_o \exp(-aT)$$

for a near zero. We also have

$$w = 0 \text{ for } x = 0, \text{ all } t.$$

The difference equation is given, e.g., by Ames (24). The computer program (in Fortran V) is given in Appendix C. We have incorporated the necessary condition for convergence (see Ref. 24, p. 323).

The general result of the computer calculation is what one would expect. The temperature at any point decreases with time. At a given

time, the T vs. r curve looks roughly like a decreasing exponential function.

For sample numerical results, we used the following values:

melting point of $A\ell_2O_3$ = 2323 K

T_o = 2500 K

density D = 4.8 g/cm^3 (Ref. 25)

heat capacity c = 197 J/mole · K (Ref. 25)

thermal conductivity k = 0.065 W/cm · K (Ref. 26)

optical absorptivity K = 0.2/cm (Ref. 27)

We find

$$N = 0.13$$

$$t^* = 1.5 \times 10^{-5} t$$

We divided x into 50 equal segments. To satisfy the convergence requirement, this means that a good value for an increment of s is 10^{-4} or less. Then we get

$$t = (140 \text{ sec/cm}^2)\ r_o^2$$

For r_o = 1 mm, incrementing t 50 times, we get a total time of 72 sec, which should be quite adequate.

Since the computer program involves dimensionless variables, a few runs for typical values of y_o are sufficient to cover all cases of interest with different substances. The results have been made available to the technical monitor at MSFC.

The PI is continuing to search for improved experimental data on substances of interest to MSFC and to study ways of expanding the applicability of the model. Any additional results will be made available to appropriate personnel at MSFC. It is intended that the results of this work be published.

REFERENCES

1. R. J. Naumann and H. W. Herring, Materials Processing in Space: Early Experiments (NASA, Washington, DC, 1980).

2. H. W. St. Clair, "An Electromagnetic Sound Generator for Producing Intense High Frequency Sound," Rev. Sci. Instrum. 12, 250 (1941).

3. L. V. King, "On the Acoustic Radiation Pressure on Spheres," Proc. Roy. Soc. (London) A147, 212 (1934).

4. J. E. Rush, "Some Characteristics of a Single-Axis Acoustic Levitation System," in 1979 NASA/ASEE Summer Faculty Fellowship Research Program, UAH Report No. 227, October, 1979 (University of Alabama in Huntsville, Huntsville, AL).

5. W. A. Oran, W. K. Witherow, B. B. Ross, and J. E. Rush, "Some Limitations on Processing Materials in Acoustic Levitation Devices," Ultrasonics Symposium Proceedings, September, 1979 (IEEE), pp. 482-486.

6. W. A. Oran, D. A. Reiss, L. H. Berge, and H. W. Parker, "Preliminary Characterization of a One-Axis Acoustic System," NASA Technical Memorandum TM-78213, January, 1979; W. A. Oran, L. H. Berge, and H. W. Parker, "Parametric Study of an Acoustic Levitation System," Rev. Sci. Instrum. 51, 626 (1980).

7. R. R. Whymark, "Acoustic Field Positioning for Containerless Processing," Ultrasonics, November, 1975.

8. P. D. Richardson, "Effects of Sound and Vibrations on Heat Transfer," Appl. Mech. Rev. 20, 201 (1967).

9. R. M. Fand and J. Kaye, "Acoustic Streaming near a Heated Cylinder," J. Acoust. Soc. Am. 32, 579 (1960).

10. J. E. Rush, C. F. Schafer, and R. L. Holland, "Analysis of SPAR VIII Single-Axis Levitation Experiment," NASA TM-82447, 59 pp.

11. L. H. Berge, W. A. Oran, and J. M. Theiss, Patent Disclosure, Patent Counsel, Marshall Space Flight Center, refer to MFS-25509; also NASA Tech Briefs, Vol. 6, No. 1, Spring 1981, p. 105.

12. F. W. Schmidt and G. S. Springer, AIAA Journal 5, 2054 (1967); 6, 1436 (1968).

13. R. Viskanta and E. E. Anderson, "Heat Transfer in Semitransparent Solids," in Advances in Heat Transfer, Vol. 11, ed. T. F. Irvine, Jr. and J. P. Hartnett (Academic Press, New York, 1975), pp. 317-441.

14. A. Chandrasekhar, Radiative Transfer (Dover Publications, Inc., New York, 1960).

15. R. Viskanta and A. L. Crosbie, "Radiative Transfer through a Spherical Shell of an Absorbing-Emitting Gray Medium," J. Quant. Spectrosc. Radiat. Transfer 7, 871-889 (1967).

16. A. L. Crosbie and H. K. Khalil, "Radiative Transfer in a Gray Isothermal Spherical Layer," J. Quant. Spectrosc. Radiat. Transfer 12, 1465-1486 (1972).

17. R. L. Lee and D. B. Olfe, "An Iterative Method for Nonplaner Radiative Transfer Problems," J. Quant. Spectrosc. Radiat. Transfer 9, 297-308 (1969).

18. A. L. Crosbie and H. K. Khalil, "Radiative Transfer in a Nongray Spherical Layer: Simplified Rectangular Model," J. Quant. Spectrosc. Radiat. Transfer 13, 359-367 (1973).

19. R. Viskanta and R. L. Merriam, "Heat Transfer by Combined Conduction and Radiation between Concentric Spheres Separated by Radiating Medium," Trans. ASME: J. Heat Transfer 90, 248-256 (1968).

20. Y. Taitel and J. P. Hartnett, "Application of Rosseland Approximation and Solution Based in Series Expansion of the Emission Power to Radiation Problems," AIAA Journal 6, 80-89 (1968).

21. E. R. G. Eckert and R. M. Drake, Jr., Analysis of Heat and Mass Transfer (McGraw-Hill, New York, 1972).

22. R. Viskanta and P. S. Lall", Transient Cooling of a Spherical Mass of High-Temperature Gas by Thermal Radiation," Trans. ASME: J. Appl. Mech. 87, 740-746 (1965); "Transient Heating and Cooling of a Spherical Mass of Gray Gas by Thermal Radiation," in M. A. Saad and J. A. Miller, eds., Proceedings of the 1966 Heat Transfer and Fluid Mechanics Institute (Stanford University Press, Stanford, Calif., 1966), pp. 181-197.

23. P. S. Lall and R. Viskanta, "Transient Energy Transfer in a Gray Radiating Gas during Expansion," Phys. Fluids 10, 98-107 (1967).

24. W. F. Ames, Nonlinear Partial Differential Equations in Engineering (Academic Press, New York, 1965).

25. E. E. Shpil'rain, et al., High Temp.-High Press. 4, 605 (1972).

26. Y. S. Touloukian, et al., Thermal Conductivity: Nonmetallic Solids, Vol. 2 of Thermophysical Properties of Matter series (IFI/Plenum, New York, 1970), p. 119.

27. Y. S. Touloukian and D. P. Dewitt, Thermal Radiative Properties: Non metallic Solids, Vol. 8 of Thermophysical Properties of Matter series (IFI/Plenum, New York, 1972), pp. 142-197.

APPENDIX A

Interim Report on Contract NAS8-33731

J. E. Rush

This is a much-expanded version of the first quarterly report on subject contract, covering work for the period June 2 - August 7 (no work done on the contract for May 8 - June 1). All the work involved the two acoustic-levitation systems at SSL/MSFC and included:

(a) instrument analysis

(b) experimental study of heat transfer from cylinders and spheres, and

(c) calculations of relevant physical quantities and comparison with published data.

Detailed data are contained in my laboratory notebook No. 2.

A. Instrument Analysis

Studies were done of the stability of the Intersonics (Model 15-1A) feedback amplifier and driver system (St. Clair generator). It was determined that a cooling fan directed at the amplifier could reduce the downward power drift of ~ 4 db in 8 min to ~0.5 db, and reduce the rapid fluctuations from $\pm$ 0.3 db to $\pm$ 0.1 db.

During the course of these studies, an instability in the driver reflector system was noted. This consists of a rapid fluctuation of ~ 4 db when the system is tuned to resonance, at ~178 db. It occurs with a concave driver and large flat reflector or a flat driver and concave reflector. It was eliminated by use of a flat driver and flat reflector or a concave driver and small flat reflector. Studies with oscilloscope and wave analyzer showed that the instability involves alternate coupling and decoupling to the first and second harmonics of the fundamental vibrating frequency (~ 15 k Hz).

Because the B & K microphones were registering 178 to 180 db for the system in resonance, and they are inaccurate beyond 170 db, an effort was made to obtain an alternate source for measurement of high sound pressure levels (SPL). With the help of John Theiss of MSFC, I obtained a strain-gauge pressure transducer, a sensor amplifier module (SAM-1) to accompany it, an oscillograph to record the signals, and a deadweight tester and 1 kHz standard source to calibrate it. The transducer was rated from 0 to 5 psi (184 db) and 0 to 40 kHz.

When the dc signal was calibrated with the deadweight tester, the transducer agreed well with the microphones at 1 kHz and 160 db, using the standard source. Unfortunately, it gave readings about 4 db higher than the microphones when placed in the field of the acoustic system, at SPL values from 155 to 180 db. The signal from the transducer was also quite different from the microphones as seen on the oscilloscope and the wave analyzer. Since the B & K microphones are known to be accurate below 170 db, I was forced to discard the strain-gauge transducer as a reliable measuring instrument for the acoustic system, and be left with no accurate measuring device for SPL values greater than 170 db. Because of instabilities at higher SPL values, this limitation may not be a practical problem.

During the above calibration process, I did wave analysis studies of the drivers with no reflector and clearly observed the sawtooth effect predicted for high SPL values.

B. Experimental Study of Heat Transfer

As a continuation of studies begun in the summer of 1979 and continued during the period September 1979 to May 1980, I constructed several heating elements and measured their heat transfer characteristics

in the acoustic field. The configurations were as given in Table 1.

TABLE 1

Coil Configurations

Shape	No. Turns	Length	Width
sphere (approx.)	5	0.4 cm	0.4 cm
cylinder	20	1.0 cm	0.3 cm
cylinder	20	1.0 cm	0.25 cm

In each case the coil was wound with B & S # 28 Nichrome wire and spot-welded to leads of B & S # 20 Kanthal wire. The coil was dipped in Sauereisen resistor cement, shaped, and allowed to dry with an iron-constantan thermocouple, made of 0.004 in. wire, imbedded approximately in the center. The leads were then inserted into a rigid ceramic holder which was taped to a rod which was mounted on a ring stand. Power was provided by a very steady ($\pm$ 0.003 A) d.c. power supply. The thermocouple leads were connected to an Omega 2168A digital thermometer which showed integer degrees.

The initial heat-transfer measurements were made in a sound field with SPL recorded at ~ 178 db by B & K 1/8" microphone (see notes about SPL measurement in Part A), using the Intersonics Model 15-1A systems. A large flat aluminum reflector was placed about 3.0 cm from the edge of a concave aluminum driver. The reflector was then raised slightly (~ 2 mm) so that the system was just far enough from resonance to avoid the large pressure fluctuations described in Part A. Several sets of data were taken with the sphere and the second cylinder, the thermocouple in the first cylinder having failed. Measurements were

also made of heat transfer from the sphere with no sound field, with no pieces of apparatus near enough to influence convective heat transfer. In the sound field, the coil was placed at the location of the first minimum below the highest maximum below the reflector, putting it approximately halfway between driver and reflector. This location should give maximum velocity of the a.c. field and maximum cooling. (This fact had been checked in earlier measurements. See laboratory notebook No. 1.)

In order to determine the effect of radiation and conduction of heat through the leads, the emissivity of the sphere was measured with an IRCON radiometer calibrated to a standard blackbody source; and thermocouples were attached at each end of a Kanthal lead with Sauereisen to determine the temperature gradient for various temperatures of the sphere. (These connections and measurements were independent of the convection measurements.)

The current to the coils was measured with a Hewlett Packard digital ammeter for all values $\leq$ 2.00 A, and the voltage across the coil was estimated by sliding probes connected to a digital voltmeter along the Kanthal leads and extrapolating to the limiting value at the points of attachment of the coil. Current values greater than 2.00 A were gotten by setting the ammeter on the power supply to a corrected value estimated from lower current readings with the digital ammeter. (Only a zero-point correction was needed).

Following the measurements at $\sim$ 178 db, measurements were made at 170, 160, 150, 140, and 130 db. Those at 170 db were made with the system configuration noted above, with the reflector adjusted for lower SPL. The remainder were made on the second amplifier-driven system, using an ALTEC 9440 A, 800 watt amplifier with oscillator and magnet

circuits constructed at MSFC. The second system was used to allow stability at lower power. To arrive at 130 db, the driving cylinder had to be firmly clamped. At 130, 140, and 150 db, the signal read by the microphone was an almost pure sine wave at 15.2 to 15.5 k Hz (depending on driving cylinder). At 160 db it was slightly distended toward a sawtooth. At 170 and 178 db it was clearly distorted. All SPL readings were taken with a 1/8" B & K microphone connected to a B & K Type 2607 measuring amplifier. The microphone was attached to a cathetometer so that it could be easily moved in and out of the sound field. All SPL readings were made at the maximum SPL point, and the microphone was removed before temperature readings were taken. All readings were rms pressure P_{rms}. The shape of the signal was determined by feeding the output of the B & K measuring amplifier into an oscilloscope.

Comparison with a good sine wave was easily made by inserting a 22.5 k Hz low-pass filter (included in the B & K unit) or by passing the signal through a wave analyzer and looking at the output of the wave analyzer on the oscilloscope. A dual trace unit on the oscilloscope was used for easy comparison.

C. Heat-Transfer Calculations

Most of the calculations were done using an HP 9835 A desktop computer located in SSL Room 215, by means of five programs - labeled SPL, QTRANS, QCOR, QMEAS, and QCAL, which I wrote and which are stored on an HP cassette. The programming language is BASIC and the programs can be easily read and interepted by anyone familiar with FORTRAN.

1. Free Convection

For free convection, Yuge (1) has obtained an empirical formula for spheres,

$$Nu = 2 + 0.392 \ Gr^{0.25}, \quad 1 < Gr < 10^5$$

where Nu is the Nusselt number and Gr is the Grashof number. His defining equations are

$$Nu = \frac{h D}{k_m}$$

and $$Gr = g D^3 \frac{\Delta t}{\nu_m^2} T_a.$$

Here D is the diameter, h the heat-transfer coefficient, k the thermal conductivity of air, g the acceleration due to gravity, Δt the difference between surface and ambient temperature, ν the kinematic viscosity of air, and T_a the absolute ambient temperature. The subscript m indicates the value at the mean between surface and ambient temperatures (the film temperature) and h is defined by

$$h = \frac{Q}{A\Delta t}$$

where Q is the heat-transfer rate and A the surface area ($= \pi D^2$).

A complete list of symbols with definitions is given at the end of this report. All Grashof numbers for my data were between 20 and 200, thus falling within Yuge's limits.

The free-convection measurements which I made agree with Yuge's formula to within 16% at all temperatures up to 550°C, even though his data only went to 70°C. In the comparison, the

radiation and conduction losses were subtracted from the measured power input to the coil. The conduction loss was obtained from

$$Q_c = 2\, k_\omega\, A_\omega \frac{\Delta t\omega}{L_\omega}$$

where A_ω is the cross-sectional area of the Kanthal wire, K_ω the thermal conductivity, and Δt_ω the temperature difference over the length L_ω. This does not allow for convective cooling of lead wires, and so overestimates the convection loss of the sphere. This fact coincides with the data, which show convection losses progressively larger than those calculated from Yuge's formula as the temperature is increased. At 550° C, the calculated radiation and conduction losses accounted for 19% and 18%, respectively, of the measured power input to the coil.

2. Convection in the Sound Field

While there do not appear to be any published data on heat transfer from spheres in an acoustic field, there are several published papers dealing with heat transfer from cylinders, either in a sound field (2-4, 6-12) or vibrated (5,7). For sufficiently long wavelengths, there should be no distinction between the effects of sound and vibration (5). Ford and Peebles (7) determined that the effects were indistinguishable for $\lambda/D \geq 12$, where λ is the effective wavelength and D is the cylinder diameter. The λ/D value for my data is 9, so some distortion might be expected when comparing them with vibration data. There are other data available in reports, which are referenced in the published papers, but it does not appear that they would add much to what has been published.

The nature of the published data is summarized in Table 1. From the table, we see that there are empirical formulae given in References 3, 5, and 9. The highest frequency is 5 k Hz, the largest SPL value is 150 db, and the highest temperature is 130° C. Thus the data themselves are not directly useful for 15 k Hz sound fields at 170 db and temperatures up to 700° C. Nevertheless we can compare our data with the empirical formulae, parametrize our data, extrapolate curves, etc., and consider what inferences might be appropriate for understanding the physical processes involved.

The empirical formulae in Refs. 3, 5, and 9 involve the following dimensionless numbers: the Grashof Number Gr, the Prantl number Pr, the vibration Mach number Ma, the vibration Reynolds number Re_v, and the Nusselt number Nu. The definitions used in the papers are

$$Gr = g D^3 \frac{\beta \Delta t}{\nu_m^2}$$

where β is the volume coefficient of thermal expansion (for an ideal gas, $\beta = \frac{1}{T}$);

$$Pr = \frac{\mu_m Cp}{k_m}$$

where μ_m is the viscosity and Cp is the specific heat at constant pressure;

$$Ma = \frac{V_s}{C}$$

where V_s is the velocity of acoustic streaming, arbitrarily chosen to be given by $V_s = a\omega$, a being the maximum

TABLE 1

Reference	Method	Frequency Range (Hz)	SPL Range (db)	λ/2D Range	Temperature Range (°C)	Comments
2	Hor. St. Wave	120	110 - 117	300	49 - 52	Temperature vs. angle
3	Hor. St. Wave	1100 - 4900	0 - 151	2 - 8	20 - 130	Pictures; graphs, formulae
4	Hor. Tr. Wave	1000 - 500	0 - 148	2 - 9	100	Pictures; Δh vs. SPL
5	Vert. Vibrations	54 - 225	0 - 150	35 - 145	35 - 125	Graphs, formulae
6	Hor. St. Wave	1500	0 - 146	6	115 - 165	Local effects
7	Hor. St. Wave & Vib.	100	136 - 150	78	50	Compare vibration & sound effects
8	Hor. St. Wave	680 - 1090	130 - 140	8 - 13	30 - 50	Local effects
9	Hor. St. Wave	645 - 672	131 - 148	13 - 14	85 - 93	L vs. Δt; formulae
10	Vert. St. Wave	710 - 1470	125 - 140	1.2 - 2.5		Local effects
11	Hor. & Vert. St. Waves	710 - 1470	125 - 140	1.2 - 2.5		Local effects
12		20 - 40	20 - 40			Local effects
This Report	Vertical St. Waves	15,000	0 - 180	4.5	20 - 700	

sound-particle amplitude of oscillation and ω the angular frequency;

$$Re_v = \frac{V_s D}{\nu_m} \qquad \text{(Ref. 5)}$$

$$Re_s = \frac{V_s' D}{\nu_m} \qquad \text{(Ref. 9)}$$

with $V_s' = (2 \pi a \omega)^2 \phi$, ϕ being determined empirically at each temperature; and

$$Nu = \frac{h}{A\Delta t}$$

as before.

There are two possible ways to define Δt. Since the sound field heats the coil even with no current supplied to it, the temperature t_o at $Q = o$ will be higher than the ambient temperature t_a. The difference is about $5°C$ for SPL = 170 and $12°$ C for SPL = 180 db. The Grashof number would normally be defined so that $Gr = 0$ when $Q = 0$. On the other hand, the forced air flow, by acoustic streaming, involves air at ambient temperature (outside the standing-wave sound field), so the Reynolds number would normally be defined for a mean temperature relative to ambient. The difference between t_o and t_a at 170 - 180 db is not trivial when one compares data plots using each one. If h is linear in one plot, it will not be linear in the other, even within experimental error.

There is also an ambiguity in the definition of the Grashof number. Ford and Kaye (3,5) state that it is evaluated at the mean film temperature, presumably implying $\beta = \beta_m = 1/T_m$. Yuge

uses $\beta = 1/T_a$. For $\Delta t < 100°$ C it made little difference, but Gr peaks at $\Delta t \approx 250°$ C using Yuge's definition and at a lower temperature with a lower value using the definition of Ford and Kaye.

The empirical formulae given in Ref. 3 are:

$$h_o = 0.245 \, (\Delta t/D)^{1/4}$$

$$h_v = [b_v \, (\Delta t \, D^3)^m/D] \; [(a \, f)^2 \, F]^n$$

$$Nu_o = 0.485 \, (Gr \, Pr)^{1/4},$$

$$Nu_v = B_v \, (Gr \, Pr)^{1/3} \; (Ma^2 F)^n$$

Here the subscript 0 implies SPL = 0, V implies SPL $\neq$ 0; h_o and h_v are in Btu/ft^2 · hr · °F; b_v and B_v vary with frequency or, more appropriately, with $\lambda/2D$; m and n vary with $\lambda/2D$; $f = 2 \pi \omega$; and F is a geometrical factor included to compensate for the different values of the amplitude a over the surface of the cylinder, so it, too, varies with $\lambda/2D$. The values of b_v and B_v are tabulated and graphed, and the values of F are graphed.

The formulae in Ref. 5 are:

$$h_o = 0.255 \, (\Delta t/D)^{1/4}$$

$$h_v = b_v \, (\Delta t/D)^{0.2} \, (af)$$

$$Nu_o = 0.495 \, (Gr \, Pr)^{1/4}$$

$$Nu_v = B_v \, (Gr \, Pr)^{0.2} \, Re_v$$

with h_o and h_v also in Btu/ft^2 • hr • °F. Thus the parameterization used by Ford and Kaye for horizontal (3) and vertical (5) standing waves is similar, except for a change from Ma to Re_s. However, the number n is about 1/3, which means that there is a change from $(af)^{2/3}$ to (af) and $(Ma)^{2/3}$ to Re_v in going from horizontal to vertical. Note that the equations for h_o and Nu_o correspond to identical situations in the two cases. In both cases, the v-subscript equations are for "fully developed vortex flows" which, according to the authors, means SPL $\gtrsim$ 146 db.

The parameterization of Ref. 9 is more complicated. Lee and Richardson (9) arrive at a formula:

$$Nu/Gr^{1/4} (1 + 1.61\ Gr^{-1/4}) = 0.372\ [\ 1 + A_i(Re_s')^2/Gr]^{1/4}$$

where Re_s (discussed above) is not calculated directly, but is replaced by means of the relation

$$B_i = (0.372)^4\ A_i \phi^2\ d^2/\nu^2\ Gr$$

with B_i determined independently at each temperature. Note that the definition of Re_s gives $Re_s \propto (af)^2$ while Ref. 5 has $Re_v \propto (af)$. Since the dependence of Re_s on (af) is never used, however, no comparison with Ref. 5 can be made. Lee and Richardson (9) claim to fit the data and Peebles (7) as well as their own, and demonstrate the fit with a graph. In Refs. 3 and 5, there is no demonstration of the degree to which the equations fit the data, except for h_v. Since the data are

shown on a graph of log h is log Δt, it would be possible to investigate the quality of fit for N_u (which I expect is rather poor) but I have not done so.

The data of this report are tabulated in my laboratory notebook No. 2, and represented in Figure 1, which is a plot of log h vs. log Δt for the data of Ford and Kaye (3,5) is shown, and we can compare data in this range for SPL = 130, 140, and 150 db. (Note: the data at 130 db are so close to those at 140 db that they are not plotted). The range of Grashof numbers in Refs. 3 and 5 is 1×10^4 to 5×10^4, while my range is 40 to 115; the range of Reynolds nubmers is 0 to 3500 for Ref. 5, 0 to 300 for my data (up to 150 db), but typical ratios $Re_v/(Gr)^{1/2}$ are of the same order of magnitude. A distinct difference is that at higher values of Δt the Grashof number peaks, then decreases.

An analysis of ordinary forced and mixed convection indicates (13) that one could expect to get

$$Nu = f(Gr, Pr, Re_v)$$

with Gr and Pr appearing as a product. Consequently, I calculated Gr, Pr, and Re_v for my data. In the calculation, I chose Yuge's definition of Gr ($\beta = 1/T_a$) and defined Δt relative to t_a. In Re_v, $v_s = (a\omega)$ is defined at t_a. By extrapolating to corresponding values of Δt at different SPL, I plotted log Nu vs. log Re_v at constant (Gr Pr), as shown in Fig. 2. Although (Gr Pr) is double valued, the curves below and above the peaks are clearly separated by different values

of Nu. Note that the data are very close to straight lines, and that the slopes are all close to the same value. For $\Delta t \lesssim 150°$ C, the slopes are about 0.56. For $\Delta t \gtrsim 300°$ C, they are about 0.52. Fig. 3 shows a plot of (Gr Pr) is Δt and Re_v is Δt. The dependence on Re_v may be compared to the data for ordinary forced convection (See Ref. 13, p. 242). For Re from 0 to 400,000, the data are well fit by

$$Nu = 0.43 + C\,(Re)^m \qquad \text{with} \qquad C = 0.48, \quad m = 0.5$$

for $0 < Re < 4{,}000$ and $c = 0.174$, $m = 0.618$ for $4{,}000 < Re < 40{,}000$. It is not possible to plot Nu vx. (Gr Pr) at constant Re_v, because there are no common values of Re_v. Consequently, I plotted $(Nu/Re_v^{0.52})$ vs. (Gr Pr) and got the graph shown in Fig. 4. The low temperature data would obviously agree better if I used $Re_v^{0.56}$; nevertheless, the trend is clear. For $\Delta t \lesssim 100°$ C we get

$$Nu \simeq 0.03 \sqrt{Re_v} \sqrt{GrPr}$$

while for $\Delta t \gtrsim 200°$ C we have

$$Nu \approx 54 \sqrt{Re_v} / (Gr\ Pr).$$

Between 100° C and 200° C there is obviously some sort of transition.

D. Further Work

The figures included in this report contain no direct indication of agreement or disagreement with the published formulae.

However, since the low temperature dependence of Nu is clearly

$$Nu \propto (Gr\ Pr)^{0.45} (Re_v)^{0.56}$$

there is no need to look for a comparison with the formulae of Ref. 5 where $Nu \propto Re_v$. There is also little hope for $Nu \propto Ma^{2/3}$ as in Ref. 3, but this should be checked, as should the complicated formula in Ref. 9. It would also be worthwhile to investigate a parameterization like

$$Nu = (Const.) + (Const.)\ (GrPr)^m\ (Re_v)^n$$

by anology with the good data on forced convection in Ref. 13. All of this can be accomplished fairly easily by computerizing the data and using a minimizing program which I have available.

A good check would be accomplished by taking additional data at 145, 155, and 165 db. The data at 178 db are suspect because we don't have a good measurement of SPL, but it would be worthwhile using the low-pass filter on the B & K amplifier and using the resulting SPL value as the correct one, just to see how the results would agree with data at 140, 150, and 160 db. The 170 db data are also suspect for purposes of comparison because the field is not close to a sine wave and we are assuming a sine wave in our parameterization.

Once the matters above have been investigated or accomplished, I plan to write a paper for publication (authors: Rush and Dean) in J. Acoust. Soc. Am. or J. Heat Transfer. I suggest the former, because they are more likely to be interested in heat transfer at high frequencies. I will, of course, try

to get a theoretical basis for the change in Nu vs. (Gr Pr) at 150° C, and for the differences between our results and others, before submitting the paper.

Following the above work, which should take about one month or perhaps during the process of the above) I plan to investigate the stability of objects in the acoustic system at room temperature, introducing specific perturbations such as air currents and reflector changes, and quantifying the observations as much as possible.

1. T. Yuge, "Experiments on heat transfer from spheres including combined natural and forced convection," J. Heat Transfer, Trans. ASME 82, 214 (1960).

2. C. T. Waker and C. E. Adams, "Thermal effects of acoustic streaming near a cylindrical obstacle", J. Acoust. Soc. Am. 813 (1959).

3. R. M. Ford and J. Kaye, "Acoustic streaming near a heated cylinder", J. Acoustic Soc. Am. 32, 579 (1960); erratum , 855 (1965); "The mechanism of sound field effects on heat transfer", J. Heat Transfer, Trans. ASME 83, 133 (1960).

4. J. P. Holman, "On the effects of sound waves on heat transfer" J. Acoust. Soc. Am. , 407 (1960); "The mechanism of sound field effects on heat transfer," J. Heat Transfer, Trans.ASME 82, 393 (1960).

5. R. M. FordandJ. Kaye, "The influence of vertical vibrations on heat transfer by free convection from a horizontal cylinder," Proceedings of the 1961 - 62 International Conference, International Developments in Heat Transfer, (1963), p. 490.

6. R. M. Ford, J. Roos, P. Cheng, and J. Kaye, "The local heat-transfer coefficient around a heated horizontal cylinder in an intense sound field", J. Heat Transfer, Trans ASME 84, 245 (1962).

7. R. M. Ford and E. M. Peebles, "A comparison of the influence of mechanical and acoustical vibrations on free convections from a horizontal cylinder", J. Heat Transfer, Trans. ASME 84, 268 (1962).

8. P. D. Richardson, "Influence of sound upon local heat transfer from a cylinder", J. Acoust. Soc. Am. 36, 2323 (1964); see also the comment on this paper by R. M. Ford, J. Acous. Soc. Am. 38, 370 (1965), and the reply by Richardson, J. Acoust. Soc. Am. 40, 1558 (1966).

9. B. H. Lee and P. D. Richardson, "Effect of sound on heat transfer from a horizontal circular cylinder at large wavelengths", J. Mech. Engng. Sci. 7, 127 (1965).

10. P. D. Richardson, "Local details of the influence of a vertical sound field on heat transfer from a circular cylinder", Proceedings of the Third International Heat Transfer Conference (, 1966), Vol. 3, p. 71.

11. P. D. Richardson, "Local effects of horizontal and vertical sound fields on natural convection from a horizontal cylinder", J. Sound vib. 10, 32 (1969).

12. J. Gosse and M. Martin, "Étude aérothermique des écoulements pulsés", 103 - 104, 887 (1970).

13. E. R. G. Eckert and R. M. Drake, Jr., Heat and Mass Transfer (McGraw-Hill, New York, 1959), Chapters 7 - 9.

Notation

a = amplitude of sound vibration

A = surface area

A_ω = cross-sectional area

c = speed of sound (at t_a)

Cp = specific heat of air at constant pressure

D = diameter of cylinder

f = frequency (sound or vibration)

g = acceleration due to gravity

Gr = Grashof number = $g D^3 \beta \Delta t / \nu_m$

h = heat transfer coefficient = $Q/A\Delta t$

k = thermal conductivity

L = length of segment of lead wire

Ma = vibration mach number = V_s/C

Nu = Nusselt number = hD/k_m

Pr = Prandtl number = $\mu_m Cp/k_m$

P_{rms} = root-mean-square sound pressure

Q = convective heat transfer rate

Re_s = streaming Reynolds number = $V_s' D/\nu_m$

Re_v = vibration Reynolds number = $V_s D/\nu_m$

SPL = sound pressure level in db (re 2×10^{-4} dyne/cm^2)

T = absolute temperature, K

t = temperature, °C

V_s = velocity amplitude = $a\omega$

V_s' = streaming speed = $(af)^2 \phi$ (Ref. 9)

β = volume coefficient of thermal expansion = 1/T for ideal gas

Δt = temperatrue difference

λ = wavelength

μ = viscosity

ν = kinematic viscosity = μ/ρ

ϕ = function of f, D, and ν such that $(af)^2 \phi$ is a characteristic streaming velocity (Ref. 9)

ρ = density of air

ω = angular frequency = $2 \pi f$.

Subscripts

o implies Q = o (this report) or SPL = o (Refs. 3,5)

m implies mean film temperature, average of surface temperature and ambient temperature

a implies ambient temperature

ω refers to Kanthal wire leads to heating coil

Fig. 1

7/28/80

Log - log

h vs. Δt

Data from ff. 67-69.

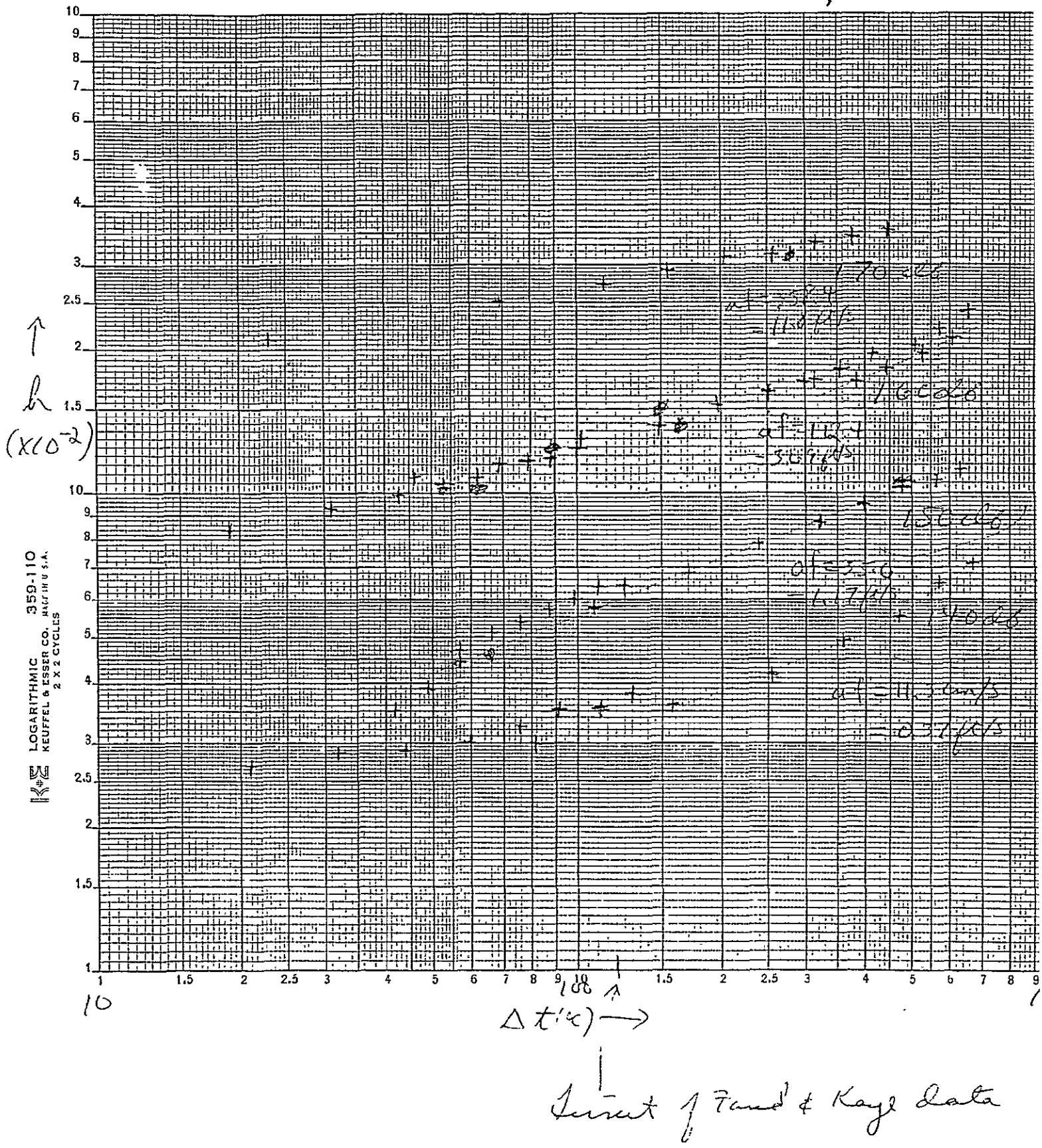

Insert 1 Found & Kayl Data

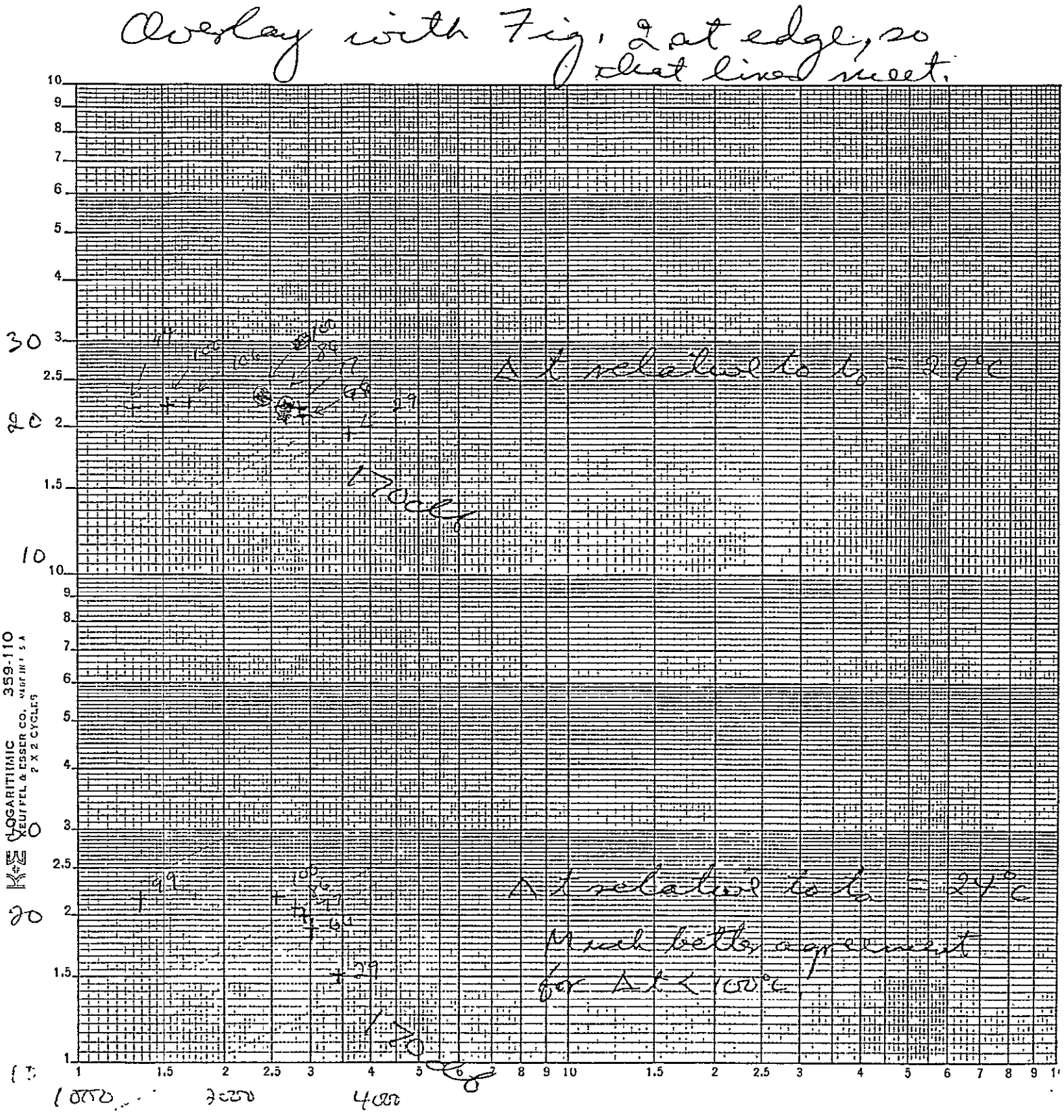

7/29/80

K·E 10 X 10 TO THE INCH • 7 X 10 INCHES
KEUFFEL & ESSER CO. MADE IN U.S.A.

46 0782

Fig. 3

Gr Pr vs. Δt & Re vs. Δt Data from pp. 67-69

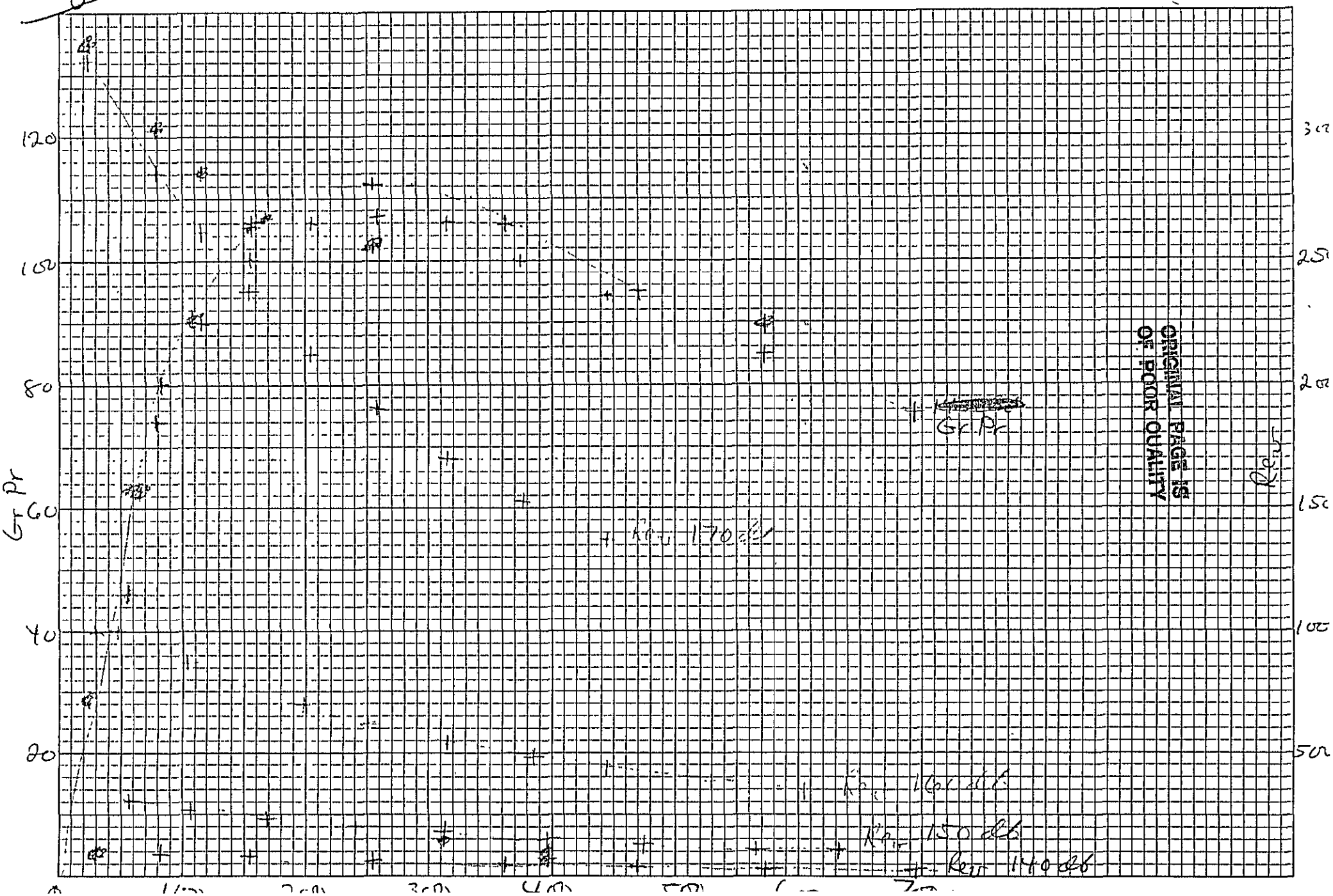

7/30/80

Data from pp. 67-6
& p. 73 (bottom,

ORIGINAL PAGE IS
OF POOR QUALITY

Fig. 4

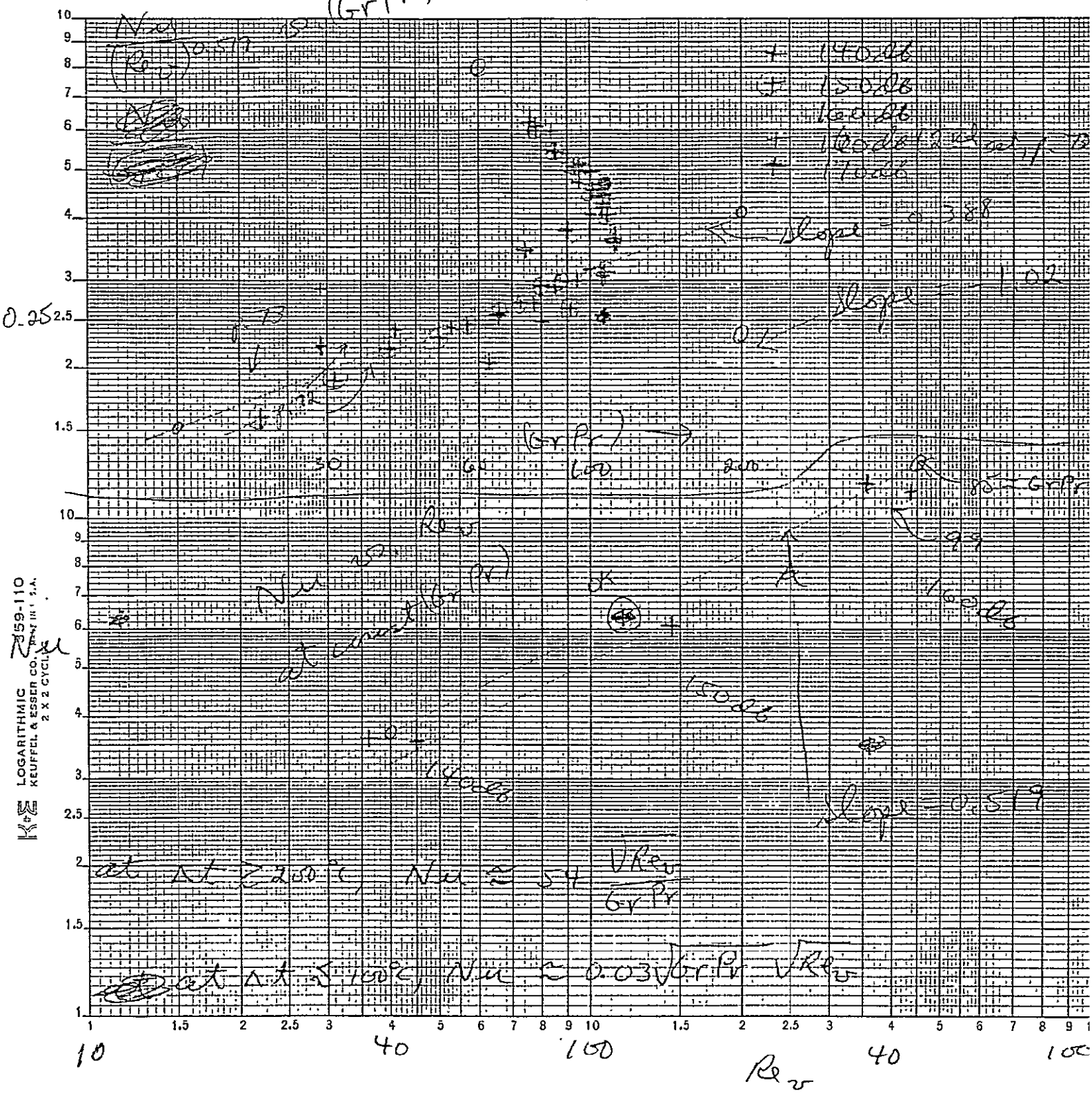

1130/80

$\frac{Nu}{(Re_v)^{0.558}}$ vs. $Gr\,Pr$ [upper] Data from pp. 72-73 & pp. 67-68 (as

Nu vs. Re_v at const. $(Gr\,Pr)$] lower

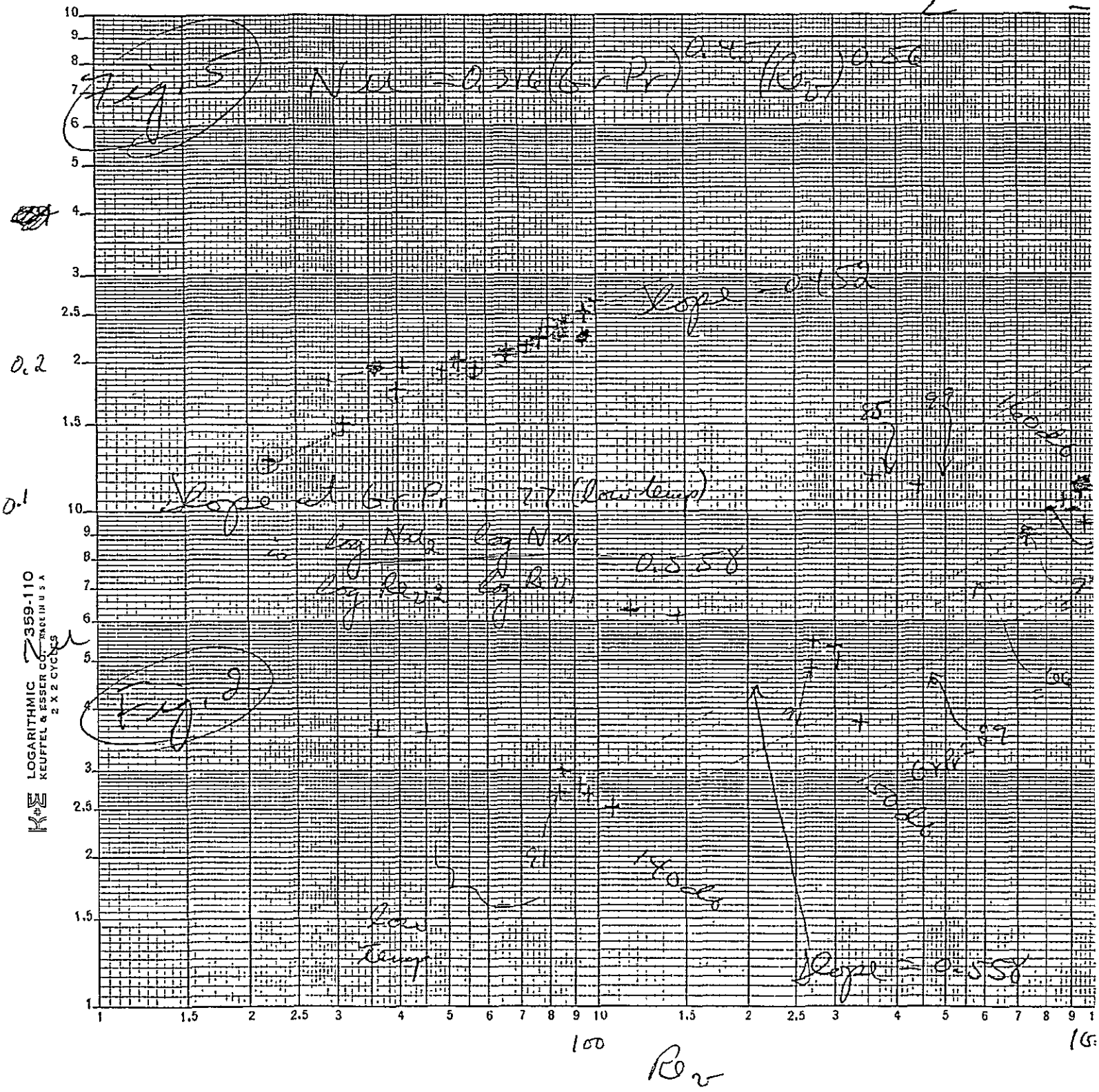

ORIGINAL PAGE IS
OF POOR QUALITY

APPENDIX B

PROPERTIES OF A CONSTRICTED-TUBE AIR-FLOW LEVITATOR

J. E. RUSH,* W. K. STEPHENS,* AND E. C. ETHRIDGE**
*Department of Physics, University of Alabama in Huntsville, Huntsville, Alabama, USA
**Space Sciences Lab, Marshall Space Flight Center, Alabama, USA

ABSTRACT

A constricted-tube gas flow levitator first developed by Berge, Oran, and Theiss shows promise both as a space-positioning device and as a levitator for ground-based work. We present results of laboratory studies which were designed to predict the behavior of the device in a low-g environment.

INTRODUCTION

There is much interest in levitation techniques which can be used in ground based research to study a number of phenomena. The effective levitation of liquid nonconductors remains an elusive goal in materials science. A constricted-tube gas flow levitator has been developed at the Marshall Space Flight Center by Berge, Oran, and Theiss [1]. Its advantages are that it is a simple levitator which is essentially orientation and gravity independent, will operate over a broad temperature range, and can be used to process both conducting and nonconducting materials. Solid spherical samples of a number of different densities at 1200°C have been successfully levitated. We have continued to study the properties of such levitators as a possible solution to this goal and as a possible levitator for low g and report here on our work to date (Sept., 1981).

The levitator consists of a constricted (quartz) tube fed at one end by a source of heated air or gas. A spherical sample is positioned by the air stream on the downstream side of the constriction, where it can be melted and resolidified without touching the tube. The primary source of heat for the sample is the air itself, although secondary sources are also being investigated. The air is heated by being passed through a furnace, by being blown past a torch, or both.

The behavior of spheres in flowing fluid in a 1g environment has been studied by many investigators. The earliest work was on spheres in free flow [2], where the drag coefficient vs. Reynolds number Re was determined. Also investigated was the pressure distribution around the sphere and the behavior of the fluid as a function of Re. A more complex situation is flow past spheres in vertical, slightly tapered tubes forming the basis of flow-meter technology. Quite a bit of work has also been done on spheres in straight tubes and pipes, both experimentally [3] and theoretically [4]. However, the only published work on spheres in duffusers which we have found is by Schmidt and Springer [5].

In a straight, vertical tube one can maintain an unstable equilibrium in the vertical direction by balancing the gravitational force with a drag force. A relatively stable equilibrium exists laterally because of a Bernoulli effect due to the radial variation in fluid velocity, coupled with a weaker Magnus force due to rotation of the sphere [6]. With a slightly tapered tube, as in a flowmeter, one can easily produce stable equilibrium, but levitation is gravity-dependent. The effect of a constriction is to supply an upstream

(Bernoulli) force which can give stable equilibrium with or without gravity.

The purpose of the work presented here is to study the properties of the levitator in order to predict its behavior in a gravity-free environment and at elevated temperatures.

EXPERIMENTAL PROCEDURE

We define the inner diameter of the tube as D_1, the constriction diameter as D_2, and the diameter of the spherical sample as d. The equilibrium position of the sample in 1g and the stable pressure were measured at each end of the tube as a function of D_2/D_1, d/D_1, shape of the constriction, flowrate through the tube, and shape of the diffuser. We also studied the net axial force on samples suspended by a wire from an electrobalance as a function of position of sample and of the variables given above. Thus we were able to map the force in the neighborhood of the expected low-g equilibrium position.

Since we are ultimately interested in levitating and melting samples at elevated temperatures we want to know how the levitation forces are affected by temperature changes. For a given tube and sample size, with the system in mechanical and thermal equilibrium, the net forces on a sample at any given point in the tube should depend only on the value of Re. By varying the fluid flow rate we can vary Re thereby modeling the effects of varying temperature on Re. Thus temperature effects can be studied by varying the flow rate.

The tubes used in these studies had an inner diameter D_1 of approximately 0.65 cm with ratios D_2/D_1 of 1/4 to 1/2. The ratios d/D_1 ranged from 1/2 to 7/8. For the shape of the constriction, we found that a simple but adequate quantitative measure was the approximate angle α of the inside surface with respect to the tube axis near the equilibrium position of the sample. The values of α ranged from 7° to 18°.

Each end of the constricted tube was attached to copper tubing by means of a plastic heat-shrinkable tubing. Fittings were mounted on each copper tube for flexible-tubing connections to pressure gauges and to a flowmeter on the upstream side. Gauge pressures were measured with and without samples inserted for the range of flow rates used (3 to 17 liters per minute). At the lower flow rates we also measured differential pressures. We also measured the variation of pressure with sample position for suspended samples. The pressure at the downstream end was never significantly different from atmospheric pressure ($\Delta P < 0.01$ psi). The precise position of the sample was read with a cathetometer.

The force measurements were made using a Cahn electrobalance. A fine wire was suspended from the electrobalance, passing through the tube, and attached to the spherical sample by means of a small bit of epoxy. In these measurements the sample material was not important, so we used assorted steel ball bearings.

In each case the suspended samples were balanced before the airflow was begun, so that the forces measured were due entirely to the airflow. The suspended samples, of course, could not rotate. Rotation would probably occur for most freely-positioned samples, but this effect would not greatly modify the restoring force (6) and would in fact improve stability.

EXPERIMENTAL RESULTS

In Table I we show some basic data for five constricted tubes which were used in these studies.

TABLE I
Basic parameters of constricted tubes

Tube Number	Inner Diameter D_1 (cm)	Constricted Diameter D_2 (cm)	Ratio D_2/D_1	Angle α
1	0.650	0.256	0.39	13°
2	0.650	0.350	0.54	9.5°
3	0.650	0.167	0.26	7°
4	0.650	0.157	0.24	18°
5	0.676	0.157	0.23	17.5°

A plot of the force, F, on a sphere in tube #5 is shown in Figure 1. Since the sphere is balanced, the force is due entirely to the fluid flow. This force is plotted against displacement of the sphere along the axis of the tube where the zero point of displacement corresponds to the point where the sphere touches the constriction and blocks the flow. The sphere used for Figure 1 had a diameter of 0.475 cm (d/D_1=0.23) and the flow rate was 13.2 liters per minute, corresponding to an average velocity of 612 cm/s at diameter D_1 (upstream).

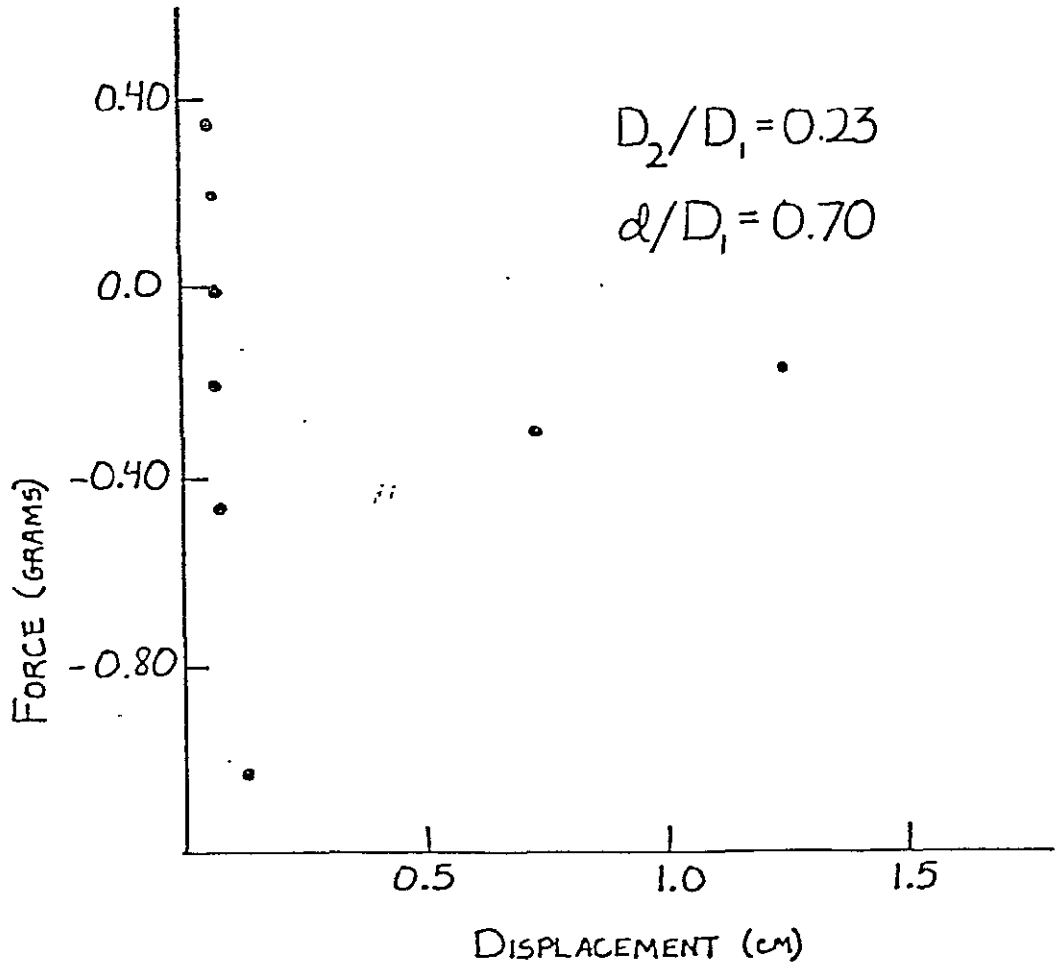

Fig. 1. Fluid force vs. displacement for balanced sphere.

Since we want stable equilibrium, we are looking for a force vs. displacement curve with a large negative slope and a broad range of positive/negative values to the left/right of zero. We also want the maximum and minimum values of the force to be reasonably large in comparison to typical sample weights. For a sample of the size used in Figure 1, which has a good d/D_1 ratio for stability, the weight for the steel sample is 440 mg. Thus the negative value for the F (10^3 mg) is quite acceptable. Since the sphere is easily levitated at this flow rate, the positive value is acceptable also. The least desirable feature of Figure 1 is the small value of the equilibrium displacement, but this can be adjusted by varying the shape of the tube.

-In Table II we summarize the results with the various tubes in terms of varying diameters of samples. In each case the flow rate chosen for comparison was based on the minimum value of the force for the range of flow rates used.

TABLE II
Best results for force minimum with each tube and sample

Tube Number	Sample [a] (Sphere)	Force Minimum (mg)	Flow Rate (ℓ/m)	Equilibrium Position (mm)
1	A	None		
	B	−380	14	
	C	None		
2	A	None		
	B	−70	5	
	C	None		
3	A	−40	4	2.0
	B	−620	9	2.5
	C	−450	14	2.5
4	A	−820	14	1.3
	B	−960	13	0.8
	C	−990	13	0.5
5	A	−990	14	0.17
	B	−1020	13	0.7
	C	−1020	13	0.6

[a] Sample diameters: A, 0.600 cm; B, 0.475 cm; C, 0.356 cm

One is also interested in the motion of the sample in the tube, primarily to avoid contamination by touching the walls and to avoid liquid sample break up. For the better diameter ratios obtained from Table II, there was no apparent motion of the sphere at equilibrium.

In Figure 2 we give some typical results for a freely levitated solid sphere at equilibrium. The larger displacements occur, of course, when the tube is inverted. From the small displacement on inversion (see Fig. 1) it is clear that one can choose flow rates such that the gravitational force becomes insignificant, as was demonstrated by Berge, Oran, and Theiss.

CONCLUSIONS

From the results given above, we conclude that the constricted-tube levitator can be used successfully as a positioning device for solid spherical samples at low g.

For operation in thermal equilibrium at high temperatures, we note that the important fluid parameter is the kinematic viscosity. If air is heated from room temperature to, say 1200°C, the kinematic viscosity increases by a factor of 14. To maintain a given value of the Reynolds number, the flow rate would

have to be increased by the same factor, for a specific geometry of tube and sample. Thus, to maintain stable equilibrium, one increases the flow rate as the air or other gas is heated. The feasibility of this process has already been demonstrated in 1 g by Berge, Oran, and Theiss.

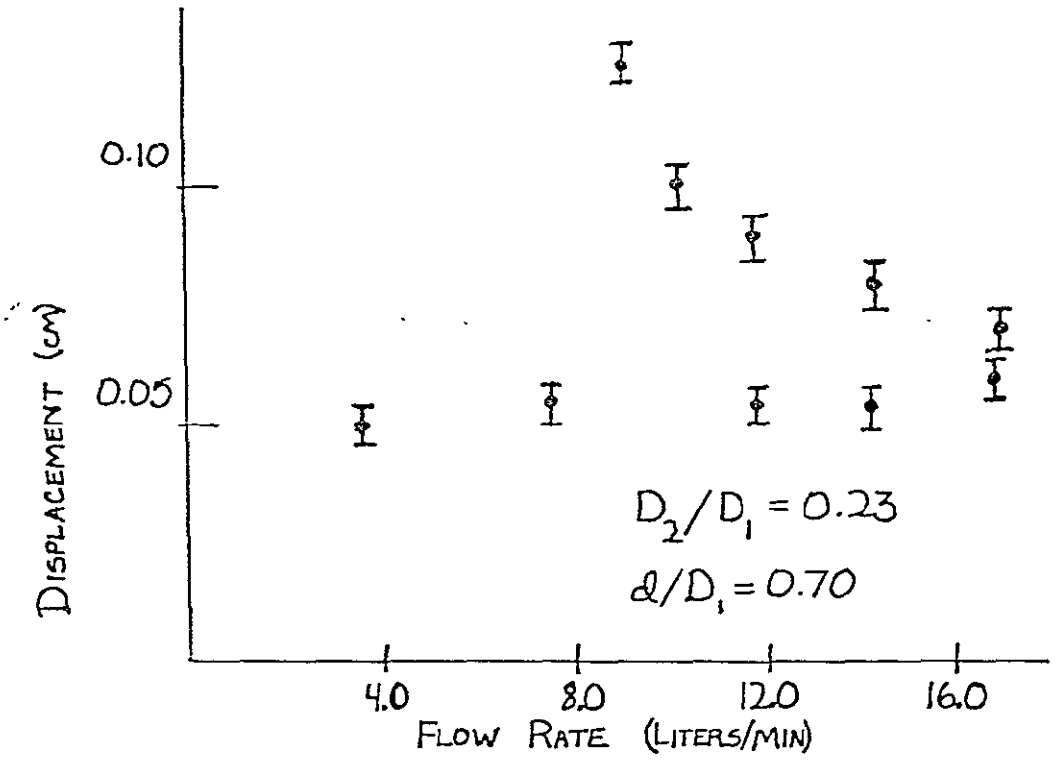

Fig. 2. Position of freely levitated steel sphere vs. flow rate at 1 g.

The other stability problem which must be considered for processing of samples is the change in shape of the spherical sample as it melts. The solution to this problem involves selecting a shape for the constriction so that the solid sample does not spin too rapidly and does not contact the tube on melting. From the data of Tables I and II, one can see that by decreasing the constriction angle (changing from Tube 5 to Tube 3) one can maintain a sufficiently large force and significantly increase the separation between tube and sample. We are currently beginning a study of the stability of melted samples at 1 g.

REFERENCES

1. L. H. Berge, W. A. Oran, and John M. Theiss, Patent Disclosure, Patent Counsel, Marshall Space Flight Center, refer to MFS-25509; also NASA Tech Briefs, Vol. 6, No. 1, Spring 1981, p. 105.

2. See, e.g., H. Schlichting, Boundary Layer Theory, Fourth ed. (McGraw-Hill, New York, 1960), p. 16.

3. G. F. Round and J. Kruyer, Chem. Engng. Sci. 29, 397 (1974); I. D. Doig, Chem. Engng. Sci. 23, 794 (1968); and references therein.

4. T. Greenstein and J. Happel, J. Fluid Mech. 34, 705 (1968); and references therein.

5. F. W. Schmidt and G. S. Springer, AIAA Journal 5, 2054 (1967); 6, 1436 (1968).

6. J. Happel and H. Brenner, A.I. Ch. E. Journal 3, 506 (1957); H. Brenner and J. Happel, J. Fluid Mech. 4, 195 (1958).

APPENDIX C

```
 RADIAT,RADIAT
1 08/31/82-09:12(,0)
    1.          REAL*8 DE,MMDEI
    2.          REAL*8 DTA
    3.          EXTERNAL MMDEI
    4.          COMMON /VARI/ THETA(50,50)      ,THETAO(50)     ,TAU(50)
    5.          COMMON /INT/  PSI(50,50)        ,PSIO(50)
    6.         1              ,ST(50)    ,TSTAR(50)          ,TPRIME(50)
    7.         1      ,X(50)     ,T(50)     ,U(50,50)
    8.         1      ,EI(100)
    9.          READ (5,101) NX, NT, M
   10.      101 FORMAT (3I5)
   11.          READ (5,102) AN, TAUO, DELTAT, ALPHA, BETA
   12.      102 FORMAT (5F10.0)
   13.          WRITE (6,151) AN, TAUO, DELTAT
   14.      151 FORMAT (//4HN = ,F5.2,4X,7HTAUO = ,F5.2,4X,10HDELTA T = ,E8.2//)
   15.          DELX = 1./NX
   16.          DELTAU = TAUO*DELX
   17.          R = DELTAT/DELX**2
   18.          NXP = NX + 1
   19.          NXPP= NX +.2
   20.          DO 201 I=1,NXPP
   21.          X(I) = (I-1)*DELX
   22.          TAU(I) = TAUO*X(I)
   23.          WRITE (6,193) TAU(I)
   24.      193 FORMAT (60X,E8.2)
   25.          GAMMA = 0.1
   26.          V = - GAMMA*X(I)
   27.          U(I,1) = EXP(V)*X(I)
   28.      201 CONTINUE
   29.          NTP = NT + 1
   30.          DO 211 J=1,NTP
   31.          T(J) = (J-1)*DELTAT
   32.          TSTAR(J) = ALPHA*T(J)
   33.          TPRIME(J) = BETA*TSTAR(J)
   34.      211 CONTINUE
   35.          NXD = 2.*NX + 4
   36.          DO 221 I=2,NXD
   37.          XA = (I-1)*DELX
   38.          TA = TAUO*XA
   39.          DTA = TA
   40.          DE = MMDEI(2,DTA,IER)
   41.          IF (IER.NE.130) GO TO 310
   42.          WRITE (6,181)
   43.      181 FORMAT (////5H ZERO)
   44.      310 CONTINUE
   45.          IF(IER.NE.131) GO TO 311
   46.          WRITE (6,182)
   47.      182 FORMAT (////8HOVERFLOW)
   48.      311 CONTINUE
   49.          EI(I) = DE
   50.          WRITE (6,191) EI(I)
   51.      191 FORMAT (30X,E8.2)
   52.      221 CONTINUE
   53.          DO 241 J=1,NTP
   54.          DO 251 I=2,NXP
   55.          THETA(I,J) = U(I,J)/X(I)
```

```
 56.      251 CONTINUE
 57.          FN = 0.0
 58.          DO 261 I=2,NXP
 59.          DO 271 K=1,NXP
 60.          TH4 = THETA(K,J)**4
 61.          KA = IABS(I-K)
 62.          KB = I + K
 63.          IF (KA.NE.0) GO TO 253
 64.          EI(KA) = 0.0
 65.      253 CONTINUE
 66.          EDIF = EI(KA) - EI(KB)
 67.          FCN = 2.*TH4*EDIF
 68.          IF (K.EQ. 1) GO TO 252
 69.          IF (K.EQ.NX) GO TO 252
 70.          FCN = 3.*FCN
 71.      252 CONTINUE
 72.          FN = FN + FCN
 73.      271 CONTINUE
 74.          TG = 0.375*DELTAU*FN
 75.          U(1,J+1) = 0.0
 76.          U(NXPP,J+1) = U(NX,J+1)
 77.          TH4 = THETA(I,J)**4
 78.          PHI = -4.*TAU(I)*TH4 + TG
 79.          FLUX = TAU0/AN*PHI
 80.          WRITE (6,192) FLUX
 81.      192 FORMAT (50X,E8.2)
 82.          UP = U(I+1,J)
 83.          UM = U(I-1,J)
 84.          UN = U(I,J)
 85.          U(I,J+1) = R*(UP-UM) + (1.-2.*R)*UN + DELTAI*FLUX
 86.      261 CONTINUE
 87.          U(1,J+1) = 3.*U(2,J+1) - 3.*U(3,J+1) + U(4,J+1)
 88.      241 CONTINUE
 89.          WRITE (6,160)
 90.      160 FORMAT (///)
 91.          WRITE (6,161)
 92.      161 FORMAT (2X,1HX,10X,1HT,11X,1HU,8X,5HTHETA/)
 93.          DO 301 J=1,NT
 94.          DO 302 I=1,NX
 95.          WRITE (6,162) X(I), T(J), U(I,J), THETA(I,J)
 96.      162 FORMAT (F5.2,4X,E8.2,4X,E8.2,4X,E12.6)
 97.      302 CONTINUE
 98.      301 CONTINUE
 99.          STOP
100.          END
```